

Hard Class Rectification for Domain Adaptation

Yunlong Zhang^a, Changxing Jing^a, Huangxing Lin^a, Chaoqi Chen^a, Yue Huang^{a,*}, Xinghao Ding^a and Yang Zou^b

^aFujian Key Laboratory of Sensing and Computing for SmartCity, School of Informatics, Xiamen University, Xiamen, Fujian, 361005, China

^bElectrical and Computer Engineering, Carnegie Mellon University, Pittsburgh, PA, 15213, U.S.A.

ARTICLE INFO

Keywords:

Unsupervised Domain Adaptation
Semi-Supervised Domain Adaptation
Pseudo-labeling
hard class problem

ABSTRACT

Domain adaptation (DA) aims to transfer knowledge from a label-rich and related domain (source domain) to a label-scare domain (target domain). Pseudo-labeling has recently been widely explored and used in DA. However, this line of research is still confined to the inaccuracy of pseudo-labels. In this paper, we reveal an interesting observation that the target samples belonging to the classes with larger domain shift are easier to be misclassified compared with the other classes. These classes are called hard class, which deteriorates the performance of DA and restricts the applications of DA. We propose a novel framework, called Hard Class Rectification Pseudo-labeling (HCRPL), to alleviate the hard class problem from two aspects. First, as is difficult to identify the target samples as hard class, we propose a simple yet effective scheme, named Adaptive Prediction Calibration (APC), to calibrate the predictions of the target samples according to the difficulty degree for each class. Second, we further consider that the predictions of target samples belonging to the hard class are vulnerable to perturbations. To prevent these samples to be misclassified easily, we introduce Temporal-Ensembling (TE) and Self-Ensembling (SE) to obtain consistent predictions. The proposed method is evaluated in both unsupervised domain adaptation (UDA) and semi-supervised domain adaptation (SSDA). The experimental results on several real-world cross-domain benchmarks, including Image-CLEF, Office-31 and Office-Home, substantiates the superiority of the proposed method.

1. Introduction

Over the last few years, Deep Neural Networks (DNNs) [15] achieved impressive performance in machine learning tasks, such as computer vision [12], speech recognition [1] and so on. Nevertheless, collecting and annotating large-scale training data in distinct domains for various applications is an expensive and labor-intensive process. Meanwhile, the applications of DNNs are greatly limited because the learned network shows poor generalization ability when it encounters new environments. Domain adaptation (DA) [23] serves as an ideal solution for addressing this problem. It has raised widespread attentions [2, 8] in the machine learning community.

Many of the existing DA methods [11, 18, 7, 8, 34, 24, 38, 33, 31] were devoted to aligning source and target features by decreasing the domain divergence, and these methods could be supported by the theoretical analysis of DA [2]. However, there are still two main limitations with these approaches: 1) methods of global alignment of source and target feature distribution cannot guarantee correctly alignment of class-level representations; and 2) global alignment methods cannot learn target-discriminative representations. Therefore, it is necessary to align the class conditional distributions of the source and target domains. However, directly pursuing the alignment of class conditional distributions is not possible due to the absence of target labels.

Pseudo-labeling [16] was first employed for semi-supervised learning tasks. Recently, pseudo-labeling was introduced into DA to solve the aforementioned issues by alternatively selecting target samples with high confident pre-

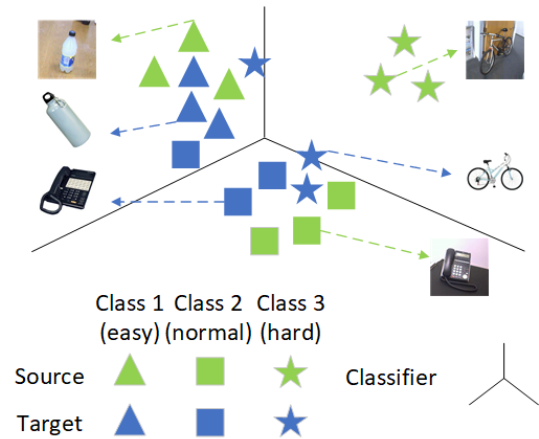


Figure 1: Hard class problem in existing pseudo-labeling based DA methods: The domain shift varies among classes. The domain shift of class 1 and class 2 is much smaller than that of class 3. Thus, in the labeling phase, class 3 in the target domain is always assigned with a label with class 1 or class 2. Therefore, class 3 is a hard class.

dictions as the pseudo-labeled target set (labeling phase) and training the model with the source domain and pseudo-labeled target set (training phase). Although pseudo-labeling is considered to be a promising paradigm, it is still limited due to the inevitable false pseudo-labels. Zhang et al. [42] demonstrated that false labels are easily fit by DNN, which harms generalization. Retraining DNN with false pseudo-labeled samples does not guarantee the generalization ability for the target domain. We further analyse the theory of DA [2] in Section 4 and demonstrate that the expected error on the target domain is determined by the false pseudo-

yhuang2010@xmu.edu.cn (Y. Huang)
ORCID(s):

labels ratio. Therefore, reducing the false pseudo-labels ratio is of crucial importance to pseudo-labeling methods. To reduce false pseudo-labels ratio, Zou et al. [46] enhanced pseudo-labeling from two aspects. 1) They introduced self-paced learning which generates pseudo-labels from easy to hard to alleviate the error accumulation of the pseudo-labels. 2) They utilized different confidence thresholds to select target pseudo-labeled set for different classes. Zou et al. [45] then introduced confidence regularization to avoid overconfident labels. Saito, Ushiku, and Harada [28] adopted two classifiers with multiview loss to label the target domain and used a fixed confidence threshold to pick up reliable pseudo-labels. Some works [40, 3, 5, 4] generate pseudo-labels in the feature space and adopt different distances to measure confidence.

In this paper, we reveal an interesting observation existing in DA problems. As shown in Figure 1. Different classes have different domain shift. Class 1, which is called easy class, has a smaller domain shift and the target samples belonging to it are very likely to be classified correctly. The model trained with source domain could generalize well on the easy class. Class 2, which is called normal class, has a moderate domain shift and a part of target samples belonging to it are classified correctly whereas others are misclassified. The previous methods [46, 45, 28, 40, 3, 5, 4], where the model could progressively learn target-discriminative representations in the process of generating pseudo-labels from easy to hard, mainly focus on the normal class. Class 3, which is called hard class, has a larger domain shift and the target samples belonging to it are easy to be misclassified. We call this the hard class problem. As far as we know, the hard class problem has not been well studied for DA tasks.

We emphasize two problems caused by the hard class problem. Firstly, The hard class problem deteriorates the transfer performance, and we analyze it in Section 4. Secondly, We remark that in many real-world applications we pay more attention to the class with the worst performance but not the average accuracy. For instance, in anomaly detection by using DA, we expect to detect the anomalies of every type, but the hard class problem causes the anomalies belonging to the hard class in the target domain could not be detected, which restrict the applications of DA. Overall, it is indispensable to consider and tackle the hard class problem for DA.

We consider and tackle the hard class problem from two aspects. Firstly, since it is difficult to classify target samples into hard class, we present a simple yet effective scheme, named Adaptive Prediction Calibration (APC), and it calibrates the predictions of target samples to promote the predictive probabilities of hard class and to attenuate the easy/normal classes. As a result, this scheme decreases the probabilities of false positives and false negatives for hard class at the same time. Secondly, the model is vulnerable to the target samples belonging to the hard class since they are far away from the source domain [35]. In spite of encountering a small perturbation (i.e., different augmentations, different classifiers), the predictions of target samples belonging to

the hard class are changed drastically. To prevent these samples to be misclassified easily, we propose two ensembling methods, Temporal-Ensembling (TE) and Self-Ensembling (SE). TE integrates the predictions of different epochs, and SE integrates the predictions of different augmentations.

In addition, the proposed schemes can be directly combined with the existing pseudo-labeling methods. In this paper, based on the CBST [46], we propose a novel pseudo-labeling framework, which combines APC, SE, and TE to alleviate the hard class problem. The proposed framework is called Hard Class Rectification Pseudo-labeling (HCRPL).

The main contributions of this work can be summarized as follows:

- i) To the best of our knowledge, we reveal the hard class problem in domain adaptation for the first time. The low pseudo-labeling accuracy in these class will results in error accumulation and then harm the final cross-domain recognition.
- ii) We tackle the hard class problem from two aspects. Firstly, since the target samples belonging to the hard class are with low accuracy in pseudo-labeling. We propose a novel APC approach to calibrate the predictions of target samples. Secondly, since target samples belonging to hard class have inconsistent predictions for small perturbations, we introduce TE and SE to improve the robustness of predictions.
- iii) We evaluate the proposed HCRPL on three public datasets under both UDA and SSDA settings. Extensive experimental results show that the proposed HCRPL achieves promising results in various DA scenarios. Especially under SSDA setting, the proposed HCRPL outperforms the state-of-the-art methods.

2. Related Work

2.1. Unsupervised Domain Adaptation

Under UDA setting, we are given a set of labeled source samples and a set of unlabeled target examples. According to Ben-David et al.'s [2] theoretical analysis of DA, the expected error for the target domain depends on three terms: the expected error on the source domain, the domain divergence, and the shared error of the ideal joint hypothesis. It can divide UDA methods into two parts. In the first part, researchers assumed that the shared error of the ideal joint hypothesis was small and mainly focused on decreasing the domain divergence. Gretton et al. [11] and Long et al. [18] reduced the domain shift by minimizing the Maximum Mean Discrepancy. Inspired by GAN [9], numerous methods [7, 8, 34, 24, 38, 33, 31] were proposed to confuse the source domain and target domain by an adversarial objective. Although the source domain and target domain are aligned well, the shared error of the ideal joint hypothesis will be large if the class conditional distributions are not aligned and separated. In the second part, researchers paid more attention to decreasing the shared error of the ideal joint hypothesis. Among the many schemes,

pseudo-labeling is a promising paradigm for reducing the third term. Saito, Ushiko, and Harada [28] adopted two classifiers to label the target set and made a constraint for the weight of two classifiers to make their different from each other. Zou et al. [46] introduced self-paced learning which generates pseudo-labels from easy to hard to alleviate the error accumulation of the pseudo-labels. Furthermore, they utilized different confidence thresholds to select target pseudo-labeled set for different classes. Zou et al. [45] introduced confidence regularization to prevent putting overconfident label belief in the wrong classes. On par with these methods that generate pseudo-labels based on predictions, some methods generate pseudo-labels in the feature space. Xie et al. [40] introduced feature centroids alignment after pseudo-labeling to DA. Chen et al. [3] proposed a progressive feature alignment that takes advantages of intra-class distribution variance in pseudo-labeling for UDA problems. Deng, Zheng, and Jiao [5] introduced the similarity-preserving constraint that can be implemented by minimizing the triplet loss with labeled source features and pseudo-labeled target features.

2.2. Semi-Supervised Domain Adaptation

Since most DA methods focus on the unsupervised setting, SSDA has not been well studied. Under SSDA setting, a set of labeled source samples, a "small" set of the labeled target set, and plenty of unlabeled target examples are given. For SSDA, the key to improving performance is learning the target-discriminative representations. In Saito et al.'s study [27], the standard UDA methods [7, 19, 29] were shown to be empirically less effective in SSDA because they fail to learn discriminative class boundaries on the target domain. By optimizing a minimax loss on the conditional entropy of unlabeled data and the task loss, Saito et al. [27] reduced the distribution gap while learning discriminative features. Motiian et al. [22] exploited the Siamese architecture to learn an embedding subspace that is discriminative and where mapped visual domains are semantically aligned and yet maximally separated. Qin et al. [25] proposed a framework consisting of a generator and two classifiers, where one is a source-based classifier and the other is a target-based classifier. The target-based classifier attempts to cluster the target features to improve intra-class density and enlarge inter-class divergence; the source-based classifier is designed to scatter the source features to enhance the smoothness of the decision boundary.

3. Methods

3.1. Preliminary

This section describes HCRPL based on the UDA setting. Under UDA setting, a source domain $\mathcal{D}_s = \{(x_i^s, y_i^s)\}_{i=1}^{m_s}$ and a target domain $\mathcal{D}_u = \{(x_i^u)\}_{i=1}^{m_u}$ are given. We define the pseudo-labeled set as $\mathcal{D}_l = \{(x_i^u, \hat{y}_i^u)\}_{i=1}^{m_l}$. Specifically, y_i^s and \hat{y}_i^u are one-hot vectors. Meanwhile, we assume that the source domain and target domain contain the same object classes, and we consider C classes. Under SSDA setting,

Algorithm 1 Overall workflow for HCRPL

Require: rounds R_s , epochs E_s , source domain \mathcal{D}_s , target domain \mathcal{D}_u , pre-trained network parameter θ .

Ensure: trained network parameter θ .

```

1: Calculate the initial ensemble predictions  $Z = \{z_i^u\}_{i=1}^{m_u}$  of target domain  $\mathcal{D}_u$  based on the pre-trained model.
2: Let training set  $\mathcal{D}_{tr} = \mathcal{D}_s$ .
3: for  $r = 1$  to  $R_s$  do
4:   for  $e = 1$  to  $E_s$  do
5:     Train network. ▷ Training phase
6:     Update the ensemble predictions  $Z$ . ▷ Predicting phase
7:   end for
8:   Select pseudo-labeled set  $\mathcal{D}_l$ . ▷ Selecting phase
9:   Update training dataset  $\mathcal{D}_{tr} = \mathcal{D}_s \cup \mathcal{D}_l$ .
10: end for
```

the source domain and labeled target set are regarded as the new source domain while the unlabeled target set is regarded as the new target domain.

The proposed HCRPL belongs to pseudo-labeling, but it is different from the standard pseudo-labeling where the target samples are predicted after every epoch but not every round. To describe the proposed HCRPL more clearly, the labeling phase is divided into predicting and selecting phases. The overall training process is given in Algorithm 1, and mainly includes three phases as follows:

- 1) Training phase: training network with the training set \mathcal{D}_{tr} .
- 2) Predicting phase: generating the ensemble predictions Z obtained from the target domain \mathcal{D}_u .
- 3) Selecting phase: selecting confident predictions as the pseudo-labeled set \mathcal{D}_l .

We define going through the process from training the network to updating \mathcal{D}_{tr} once as one round. The proposed APC, TE, and SE are included in the predicting phase. The overall training process along with APC, TE, and SE are introduced below.

3.2. Adaptive Prediction Calibration

The process of APC is shown in Figure 2 top. The target domain \mathcal{D}_u is first fed into the trained model to obtain the predictions $P = \{p_i^u\}_{i=1}^{m_u}$. Then, we define a ratio R of prior class distribution $q(y)$ to the predictive class distribution $p(y)$ as follows

$$R = q(y) \oslash p(y), \quad (1)$$

where $q(y) = \frac{1}{m_s} \sum_{i=1}^{m_s} y_i^s$, $p(y) = \frac{1}{m_u} \sum_{i=1}^{m_u} p_i^u$ and \oslash means element-wise division, and R is a C -dimensional vector with i -th dimension being the difficulty degree belonging to i -th class. Finally, we calibrate predictions P by

$$P \leftarrow \{\text{Normalization}(R \odot p_i^u)\}_{i=1}^{m_u}, \quad (2)$$

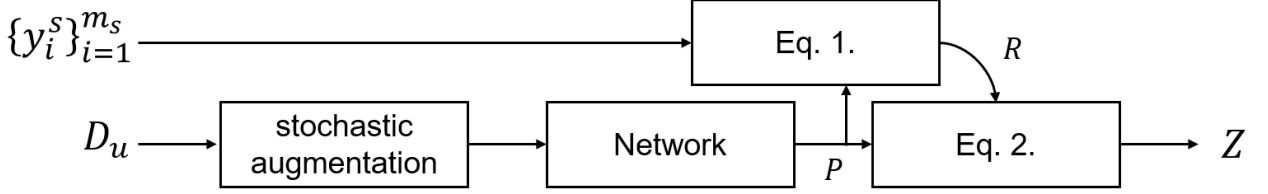
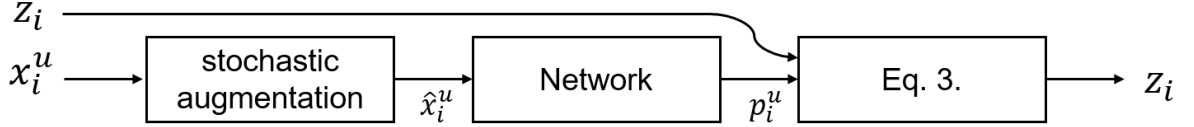
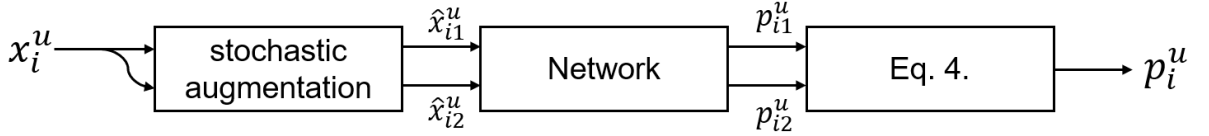
APC**TE****SE**

Figure 2: Structure of the training pass in HCRPL. Top: APC. Middle: TE. Bottom: SE. the details of Eq.1., Eq.2., Eq.3. and Eq.4. are show in Equal 1, 2, 3 and 4.

where $\text{Normalization}(x) = \frac{x}{\sum_i x_i}$ and \odot means element-wise multiplication. Intuitively, we calibrate P by R . For a certain class c , if the predictive probability of class c is small, which means that class c is a hard class, the APC will increase the probabilities of classifying target samples into class c .

3.3. Temporal-Ensembling and Self-Ensembling

Two ensembling methods, TE and SE, are adopted to improve the robustness of predictions of target samples. For TE, integrating predictions of multiple classifiers is considerable to obtain consistent predictions. Different from that Saito, Ushiku, and Harada [28] constructed two classifiers with multiview loss, in this paper, we adopt the temporal-ensembling based method which views the trained model after different epochs as different classifiers and there is no need to construct multiple classifiers. As shown in Figure 2 middle, we evaluate the target domain after every epoch and update the ensemble predictions z_i by Exponential Moving Average (EMA). The EMA can be formulated as

$$z_i \leftarrow \alpha z_i + (1 - \alpha) p_i^u. \quad (3)$$

The EMA could memorize all predictions and place a greater weight on the most recent predictions. α is the EMA momentum, and recent predictions will have a higher proportion with a lower α . If $\alpha = 0$, then the ensemble predictions z_i are equal to the current predictions p_i^u . Specifically, the ensemble predictions z_i are used to select pseudo-labeled samples in the selecting phase.

For SE, we integrate the predictions of two different augmentations. As shown in Figure 2 bottom, we feed the target samples into the trained model twice with different

stochastic augmentations and obtain predictions p_{i1}^u and p_{i2}^u . Then, the ensemble predictions p_i^u are calculated by

$$p_i^u = \frac{p_{i1}^u + p_{i2}^u}{2}. \quad (4)$$

TE and SE are somewhat similar to Π -model [14] and Mean Teacher [6, 37]. These methods took the difference of the predictions of different epochs and augmentations as a regularization term to constrain the model. Our aim is different from these methods. We expect to improve the robustness of predictions by enforcing the predictions of different augmentations and epochs consistency.

3.4. Overall Training Process

The details of the training, predicting, and selecting phases are described below.

In the training phase, the network is trained with training dataset D_{tr} . In the first round, we view D_s as D_{tr} and subsequently update D_{tr} with the pseudo-labeled target set D_l and source domain D_s . The training objective is defined as

$$L = \frac{1}{m_s + m_t} \left(\sum_{i=1}^{m_s} H(y_i^s, p_i^s) + \sum_{i=1}^{m_t} H(\hat{y}_i^u, p_i^u) \right), \quad (5)$$

where $H(p, q)$ is the standard cross-entropy loss function. With the number of pseudo-labeled target samples increasing, the network learns more of the target-discriminative representations and gradually enhances the transfer performance in the target domain.

In the predicting phase, our aim is improve the accuracy and robustness of predictions, especially for the hard class.

Algorithm 2 Details of the prediction process

Require: ensemble predictions shadow value Z , prior class distribution $q(y)$, target domain D_u , network parameter θ , EMA momentum α .

Ensure: updated ensemble predictions shadow value Z .

```

1: Let  $P_1 = \emptyset, P_2 = \emptyset$ .
2: for  $i = 1$  to  $m_u$  do
3:    $\hat{x}_{i1}^u = \text{Augment}(x_i^u)$ 
4:    $\hat{x}_{i2}^u = \text{Augment}(x_i^u)$ 
5:    $P_1 \leftarrow P_1 + p_{i1}^u$   $\triangleright p_{i1}^u = p(y|\hat{x}_{i1}^u, \theta)$ 
6:    $P_2 \leftarrow P_2 + p_{i2}^u$   $\triangleright p_{i2}^u = p(y|\hat{x}_{i2}^u, \theta)$ 
7: end for
8:  $p(y) = \frac{1}{2m_u}(\sum_{i=1}^{m_u}(p_{i1}^u + p_{i2}^u))$ 
9:  $R = q(y) \otimes p(y)$ 
10:  $P_1 \leftarrow \{\text{Normalization}(R \otimes p_{i1}^u)\}_{i=1}^{m_u}$ 
11:  $P_2 \leftarrow \{\text{Normalization}(R \otimes p_{i2}^u)\}_{i=1}^{m_u}$ 
12:  $P = \frac{P_1 + P_2}{2}$ 
13:  $Z \leftarrow \alpha Z + (1 - \alpha)P$ 
14: return  $Z$ 

```

We propose the APC, TE, and SE to adjust the predictions of target samples. The overall workflow pseudo-code for the predicting phase is given in Algorithm 2. The predicting phase can be split into five parts: Firstly, the target set is augmented twice and the corresponding predictions P_1, P_2 are obtained (Line 2-7). Secondly, the difficulty ratio R of prior class distribution $q(y)$ to predictive class distribution $p(y)$ is calculated (Line 8-9). Thirdly, the APC is applied to calibrate predictions P_1, P_2 (Line 10-11). Fourthly, the average predictions $\frac{P_1 + P_2}{2}$ are calculated (Line 12). Finally, the ensemble predictions Z are updated by EMA (Line 13).

In the selecting phase, we select the predictions of target samples with higher confidence as pseudo-labels. CBST [46] considers that different classes should have different confidence thresholds and dynamically adjusts thresholds to generate pseudo-labels from easy to hard. The class-balanced self-training solver can be formulated as

$$\hat{y}_{ic}^u = \begin{cases} 1, & \text{if } c = \underset{c}{\operatorname{argmax}} \frac{z_{ic}^u}{\exp(-k_c)}, \\ \frac{z_{ic}^u}{\exp(-k_c)} > 1. \\ 0, & \text{otherwise.} \end{cases} \quad (6)$$

Here, z_i^u means the ensemble predictions of i -th sample in the target domain. z_{ic}^u means the ensemble probability for the c -th class in z_i^u . k_c for each class c is determined by a single portion parameter p that indicates how many samples to select in the target domain. Practically, p is gradually increased to select more pseudo-labeled samples for each round. For a detailed algorithm, we recommend reading Algorithm 2 in Zou et al's paper [46].

4. Theoretical Analysis

This section explains why the hard class problem harms the transfer performance, and our explanation is based on

Ben-David et al's [2] theoretical analysis of DA.

Theorem 4.1. *Let H be the hypothesis class. Given two different domains S and T , we have*

$$\forall h \in H, R_T(h) \leq R_S(h) + \frac{1}{2}d_{H\Delta H}(S, T) + C, \quad (7)$$

where the expected error on the target samples $R_T(h)$ are bounded by three terms: (1) the expected error on the source domain, $R_S(h)$; (2) $d_{H\Delta H}(S, T)$ is the domain divergence measured by a discrepancy distance between the source domain distribution S and the target domain distribution T w.r.t. a hypothesis set H ; and (3) the shared error of the ideal joint hypothesis C . $C = \min_{h \in H}[\epsilon_S(h, f_S) + \epsilon_T(h, f_T)]$, and $\epsilon_S(h)$ is the expected error of h on the source domain.

In this study, we focus on the third term that is the shared error of the ideal joint hypothesis C . According to triangle inequality for classification error [2], that is, for any labeling functions f_1, f_2 and f_3 , we have $\epsilon(f_1, f_2) \leq \epsilon(f_1, f_3) + \epsilon(f_2, f_3)$, we could have

$$\begin{aligned} C &= \min_{h \in H} \epsilon_S(h, f_S) + \epsilon_T(h, f_T) \\ &\leq \min_{h \in H} \epsilon_S(h, f_S) + \epsilon_T(h, f_{T_1}) + \epsilon_T(f_{T_1}, f_T), \end{aligned} \quad (8)$$

$\epsilon_S(h, f_S) + \epsilon_T(h, f_{T_1})$ denotes the shared error of h^* on the source domain S and pseudo-labeled set D_l and is minimized by the training model with the source domain S and pseudo-labeled set D_l . $\epsilon_T(f_{T_1}, f_T)$ denotes the false pseudo-labels ratio. Overall, the expected error on the target domain is determined by the false pseudo-labels ratio.

Next, we combine the hard class problem with the false pseudo-labels ratio. Firstly, few target samples are classified into hard class, and the model can not learn target discriminative representations for the hard class. Further, fewer target samples are classified into hard class, which aggravates the hard class problem. Secondly, target samples belonging to the hard class are misclassified into the other classes, which causes misaligning and negative transfer. Overall, the hard class problem will cause error accumulation and increase the false pseudo-labels ratio.

5. Experiments

5.1. Datasets

5.1.1. ImageCLEF-DA

ImageCLEF-DA¹ is a benchmark dataset for ImageCLEF 2014 DA challenges. Three domains, including Caltech-256 (C), ImageNet ILSVRC 2012 (I), and Pascal VOC (P), share 12 categories. Each domain contains 600 images and 50 images for each category.

5.1.2. Office-31

Office-31 [26] is a standard benchmark for DA tasks. The dataset contains 4110 images of 31 categories collected

¹<http://imageclef.org/2014/adaptation>



Figure 3: Example images in ImageCLEF-DA, Office-31, and Office-Home

from three domains: Amazon (A), Webcam (W), and Dslr (D). Under SSDA setting, we followed the settings used by Saito et al. [27] and then evaluated the proposed method on the task between $W \rightarrow A$ and $D \rightarrow A$.

5.1.3. Office-Home

Office-Home [39] is a more challenging DA dataset compared to Office-31. It consists of 15500 images from 65 categories and is organized into four domains: Art (Ar), Clipart (Cl), Product (Pr), and Real-world (Rw).

We show the examples of three datasets in Figure 3. We can see different classes have different domain shift. For example, the examples of class 'Horse' in different domains are similar each other whereas the examples of class 'Bike' in different domains varies a lot.

5.2. Baselines

5.2.1. Unsupervised Domain Adaptation

Under UDA setting, we evaluated HCRPL with **ResNet-50** [12]. We compared the proposed HCRPL with the latest methods, including Reverse Gradient (**RevGrad**) [7], Joint Adaptation Networks (**JAN**) [20], Class-Balanced Self-Training (**CBST**) [46], Confidence Regularized Self-Training (**CRST**) [45], **CDAN** [19], **SAFN** [41], Domain-Symmetric Networks (**SymNets**) [44], Domain adversarial neural network (**DANN**) [8], Discriminative Adversarial Domain Adaptation (**DADA**) [36], **MDD** [43], Maximum Classifier Discrepancy (**MCD**) [30] and Cycle-consistent Conditional Adversarial Transfer Networks (**3CATN**) [17].

5.2.2. Semi-Supervised Domain Adaptation

In the SSDA experiment, we evaluated the proposed model with **AlexNet** [13] and **VGG16** [32]. The proposed model was compared with Domain adversarial neural network (**DANN**) [8], **CDAN** [19], **ENT** [10], Adversarial dropout regularization (**ADR**) [29], and the Minimax Entropy (**MME**) [27].

5.3. Implementation Details

The proposed HCRPL was implemented with PyTorch². For a fair comparison, our backbone network was the same as the competitive methods. For AlexNet, we replace the last full-connected layer with a randomly initialized bottleneck layer which consist of two full-connected layers: $4096 \rightarrow C$. For VGG and ResNet, we replace the last full-connected layer with a randomly initialized C -way classifier layer. It was pre-trained on ImageNet and then fine-tuned using SGD with a weight decay of 5×10^{-4} , momentum of 0.9, and batch size of 32. Likewise, we used horizontal-flipping and random-cropping based data augmentation for all the training data. For the pseudo-labeling setting, we set the total number of pseudo-labeling rounds to be 30, each with 20 epochs. In the r -th round, we choose the top $p\%$ of the highest confidence target samples within each category, and $p = \min(r * 5 + 10, 90)$. In the first round, the network was trained with labeled data (source domain in UDA; source domain and labeled target data in SSDA) with a learning rate of 5×10^{-5} or 1×10^{-4} . Furthermore, it was then retrained in the subsequent rounds with a learning rate of 1.5×10^{-5} . We set the EMA momentum α to 0.95. Under SSDA setting, we added a few-shot module to AlexNet and VGG16 like Saito et al. [27] for better comparison with MME.

5.4. Results

5.4.1. Unsupervised domain adaptation

The transfer performances on the Office-Home, Office-31, and ImageCLEF-DA under UDA setting are shown in Table 1, 2, and 3, respectively. For Office-Home, the result is shown in Table 1, and HCRPL outperforms the best performance by 2.8% on average and achieves state-of-the-art performance on most tasks. It should be noted that the proposed framework has a larger improvement on the transfer

²<https://pytorch.org/>

Table 1
ResNet50-based approaches on Office-Home under UDA setting (%)

Method	Ar Cl	Ar Pr	Ar Rw	Cl Ar	Cl Pr	Cl Rw	Pr Ar	Pr Cl	Pr Rw	Rw Ar	Rw Cl	Rw Pr	Avg
ResNet50 [12]	34.9	50.0	58.0	37.4	41.9	46.2	38.5	31.2	60.4	53.9	41.2	59.9	46.1
RevGrad [7]	45.6	59.3	70.1	47.0	58.5	60.9	46.1	43.7	68.5	63.2	51.8	76.8	57.6
CBST [46]	51.4	74.1	78.9	56.3	72.2	73.4	54.4	41.6	78.8	66.0	48.3	81.0	64.7
CDAN+E [19]	50.7	70.6	76.0	57.6	70.0	70.0	57.4	50.9	77.3	70.9	56.7	81.6	65.8
SAFN [41]	52.0	71.7	76.3	64.2	69.9	71.9	63.7	51.4	77.1	70.9	57.1	81.5	67.3
SymNets [44]	47.7	72.9	78.5	64.2	71.3	74.2	64.2	48.8	79.5	74.5	52.6	82.7	67.6
MDD [43]	54.9	73.7	77.8	60.0	71.4	71.8	61.2	53.6	78.1	72.5	60.2	82.3	68.1
HCRPL (proposed)	59.5	76.8	80.8	67.2	76.7	78.9	63.2	53.1	81.2	72.3	57.2	84.4	70.9

Table 2
ResNet50-based approaches on Office-31 under UDA setting (%)

Method	A \rightarrow W	D \rightarrow W	W \rightarrow D	A \rightarrow D	D \rightarrow A	W \rightarrow A	Avg
ResNet50 [12]	68.4 \pm 0.2	96.7 \pm 0.2	99.3 \pm 0.1	68.9 \pm 0.2	62.5 \pm 0.3	60.7 \pm 0.3	76.1
DANN [8]	82.0 \pm 0.4	96.9 \pm 0.2	99.1 \pm 0.1	79.7 \pm 0.4	68.2 \pm 0.4	67.4 \pm 0.5	82.2
CBST [46]	87.8 \pm 0.8	98.5 \pm 0.1	100.0 \pm 0.0	86.5 \pm 1.0	71.2 \pm 0.4	70.9 \pm 0.7	85.8
MCD [30]	89.6 \pm 0.2	98.5 \pm 0.1	100.0 \pm 0.0	91.3 \pm 0.2	69.6 \pm 0.3	70.8 \pm 0.3	86.6
CRST [45]	89.4 \pm 0.7	98.9 \pm 0.4	100.0 \pm 0.0	88.7 \pm 0.8	72.6 \pm 0.7	70.9 \pm 0.5	86.8
SAFN+ENT [41]	90.1 \pm 0.8	98.6 \pm 0.2	99.8 \pm 0.0	90.7 \pm 0.5	73.0 \pm 0.2	70.2 \pm 0.3	87.1
CDAN+E [19]	94.1 \pm 0.1	98.6 \pm 0.1	100.0 \pm 0.0	92.9 \pm 0.2	71.0 \pm 0.3	69.3 \pm 0.3	87.7
SymNets [44]	90.8 \pm 0.1	98.8 \pm 0.3	100.0 \pm 0.0	93.9 \pm 0.5	74.6 \pm 0.6	72.5 \pm 0.5	88.4
MDD [43]	94.5 \pm 0.3	98.4 \pm 0.1	100.0 \pm 0.0	93.5 \pm 0.2	74.6 \pm 0.3	72.2 \pm 0.1	88.9
3CATN [17]	95.3 \pm 0.3	99.3 \pm 0.5	100.0 \pm 0.0	94.1 \pm 0.3	73.1 \pm 0.2	71.5 \pm 0.6	88.9
DADA [36]	92.3 \pm 0.1	99.2 \pm 0.1	100.0 \pm 0.0	93.9 \pm 0.2	74.4 \pm 0.1	74.2 \pm 0.1	89.0
HCRPL (proposed)	95.9 \pm 0.2	98.7 \pm 0.1	100.0 \pm 0.0	94.3 \pm 0.2	75.0 \pm 0.4	75.4 \pm 0.4	89.9

tasks with larger domain shift. For example, the tasks Ar \rightarrow Cl and Cl \rightarrow Ar have poor generalization ability on target domain, and HCRPL has an improvement over MDD by 5.4% on Ar \rightarrow Cl and 7.2% on Cl \rightarrow Ar. For Office-31, we report the averages and standard deviations of the evaluation results over 3 runs. HCRPL outperforms all the other methods on A \rightarrow W, A \rightarrow D, D \rightarrow A, D \rightarrow A, and the average of all the sub-tasks. For ImageCLEF-DA, HCRPL outperforms all the other methods on I \rightarrow P, P \rightarrow I, C \rightarrow I, C \rightarrow P, P \rightarrow C, and the average of all sub-tasks.

5.4.2. Semi-supervised domain adaptation

We show results on Office-31 and Office-Home under SSDA setting. As shown in Table 4 and 6, the proposed HCRPL achieves the state-of-the-art performance on all settings (e.g., different networks, different labeled target sample size) and sub-tasks. Specifically, on Office-31 1-shot, HCRPL outperforms MME by 5.8% using AlexNet. As a reference, MME outperforms S+T by 6.3% under the same setting. Training with AlexNet is more challenging than VGG, but HCRPL improves more on AlexNet, which also proves the effectiveness of HCRPL in challenging scenarios. Similarly, under SSDA setting, HCRPL has a larger improvement on the tasks with larger domain shift.

5.4.3. Comparisons with CBST

Tables 1, 2, 3, 4 and 6 also provide the results of CBST on different tasks. HCRPL not only outperforms on all tasks but also improves performance by a large margin compared to CBST, which implies that HCRPL promotes overall compared to CBST. Specifically, we discover that the performance improvements are more visible on hard tasks (for example, A \rightarrow D in Office-31), which illustrates that the hard class problem will further deteriorate the performance of pseudo-labeling in the case of large domain shift, and the proposed HCRPL could alleviate it.

5.5. Ablation Study

We conduct the ablation study under four different settings. The results are shown in Table 5. As shown, the APC module plays the most important role in HCRPL. The large performance degradation without APC indicates that calibrating the predictions of target samples is effective to improve transfer performance. Besides, SE and TE could further improve performance by improving the robustness of predictions. Moreover, the performance of CBST is much lower than the proposed methods, which proves that the hard class problem deteriorates transfer performance dramatically and the proposed schemes are effective.

The proposed effect can be further demonstrated by the accuracy of the pseudo-labels during the training process.

Table 3
Results on the ImageCLEF-DA dataset under UDA setting(%)

Method	I → P	P → I	I → C	C → I	C → P	P → C	Avg
ResNet50 [12]	74.8	83.9	91.5	78.0	65.5	91.2	80.7
DANN [8]	75.0	86.0	96.2	87.0	74.3	91.5	85.0
MCD [30]	77.3	89.2	92.7	88.2	71.0	92.3	85.1
JAN [20]	76.8	88.0	94.7	89.5	74.2	91.7	85.8
CBST [46]	77.8	91.7	96.2	91.1	75.0	93.9	87.6
CDAN+E [19]	77.7	90.7	97.7	91.3	74.2	94.3	87.7
SAFN [41]	78.0	91.7	96.2	91.1	77.0	94.7	88.1
HCRPL	78.2	92.9	96.6	92.3	77.5	95.8	88.9

Table 4
Results on the Office-31 datasets under SSDA setting(%)

Network	Method	W → A		D → A	
		1-shot	3-shot	1-shot	3-shot
AlexNet	S+T	50.4	61.2	50.0	62.4
	DANN [8]	57.0	64.4	54.5	65.2
	ADR [29]	50.2	61.2	50.9	61.4
	CDAN [19]	50.4	60.3	48.5	61.4
	ENT [10]	50.7	64.0	50.0	66.2
	MME [27]	57.2	67.3	55.8	67.8
	CBST [46]	57.5	66.0	54.8	63.9
	HCRPL	63.2	69.9	61.4	70.0
VGG	S+T	57.4	62.9	68.7	73.3
	ENT [10]	51.6	64.8	70.6	75.3
	CDAN [19]	55.8	61.8	65.9	72.9
	ADR [29]	57.4	63.0	69.4	73.7
	DANN [8]	60.0	63.9	69.8	75.0
	MME [27]	62.7	67.6	73.4	77.0
	CBST [46]	71.4	76.6	70.8	76.2
	HCRPL	74.6	77.2	74.0	77.8

Table 5
Ablation study under four settings. U and S denote UDA and SSDA, respectively; and R and A denote ResNet50 and AlexNet, respectively. 1 means 1-shot. w/o means without.

Methods	CI→Ar	A→W	Rw→CI	D→A
	UR	UR	SA1	SV1
CBST	56.5	87.0	39.7	62.4
HCRPL w/o APC	62.3	88.6	40.4	65.1
HCRPL w/o SE	66.6	92.5	45.3	68.8
HCRPL w/o TE	66.2	93.1	44.7	69.1
HCRPL (full)	67.2	95.9	46.0	70.0

Due to the limited space, only the corresponding results of CI → Ar and A → W under UDA setting are provided in Figure 4. APC substantially improves the accuracy of pseudo-labels. SE and TE improve the accuracy of pseudo-labels at the beginning of training process and then continue to work during the whole training process. Meanwhile, it is found that the accuracy of the pseudo-labels varies similarly without SE or TE, which illustrates that they perform similar

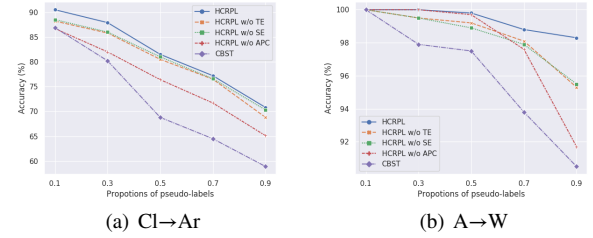


Figure 4: The accuracy of pseudo-labels with respect to the ratio of pseudo-labels of different ablation studies on (a) Office-Home CI → Ar, ResNet-50, and UDA settings; (b) Office-31 A → W, ResNet-50, and UDA settings.

roles. Moreover, the close relationship between the transfer performance and the accuracy of pseudo-labels empirically proves that the false pseudo-labels ratio determines the expected error on the target domain in pseudo-labeling.

5.6. Analysis

5.6.1. Exploring the hard class problem.

We train CBST and HCRPL on Office-31 W → A under UDA setting. Figure 5 (a-d) show visualizations of the confusion matrix for the classifier learnt by CBST, HCRPL without APC, HCRPL without SE and TE and HCRPL. As shown in Figure 5(a), few target samples are classified into the 28-th class ('Stapler') for the classifier learned by CBST, which confirms the existence of the hard class problem and indicates that Stapler is a hard class.

We first analyze the impact of APC on the hard class problem. Compared to Figure 5 (a) and (b), Figure 5 (c) and (d) show the results of adding APC to CBST and HCRPL without SE and TE. Obviously, APC could alleviate the hard class problem. Then, we analyze the impact of SE and TE on the hard class problem. Compared Figure 5 (a) and (b), only adding SE and TE has no difference to the hard class problem. This result is quite reasonable, because only improve the robustness of predictions could not increase the probabilities of classifying target samples into the hard class. Compared Figure 5 (c) and (d), adding SE and TE after APC could further alleviate the hard class problem. Since SE and TE could improve the robustness of predic-

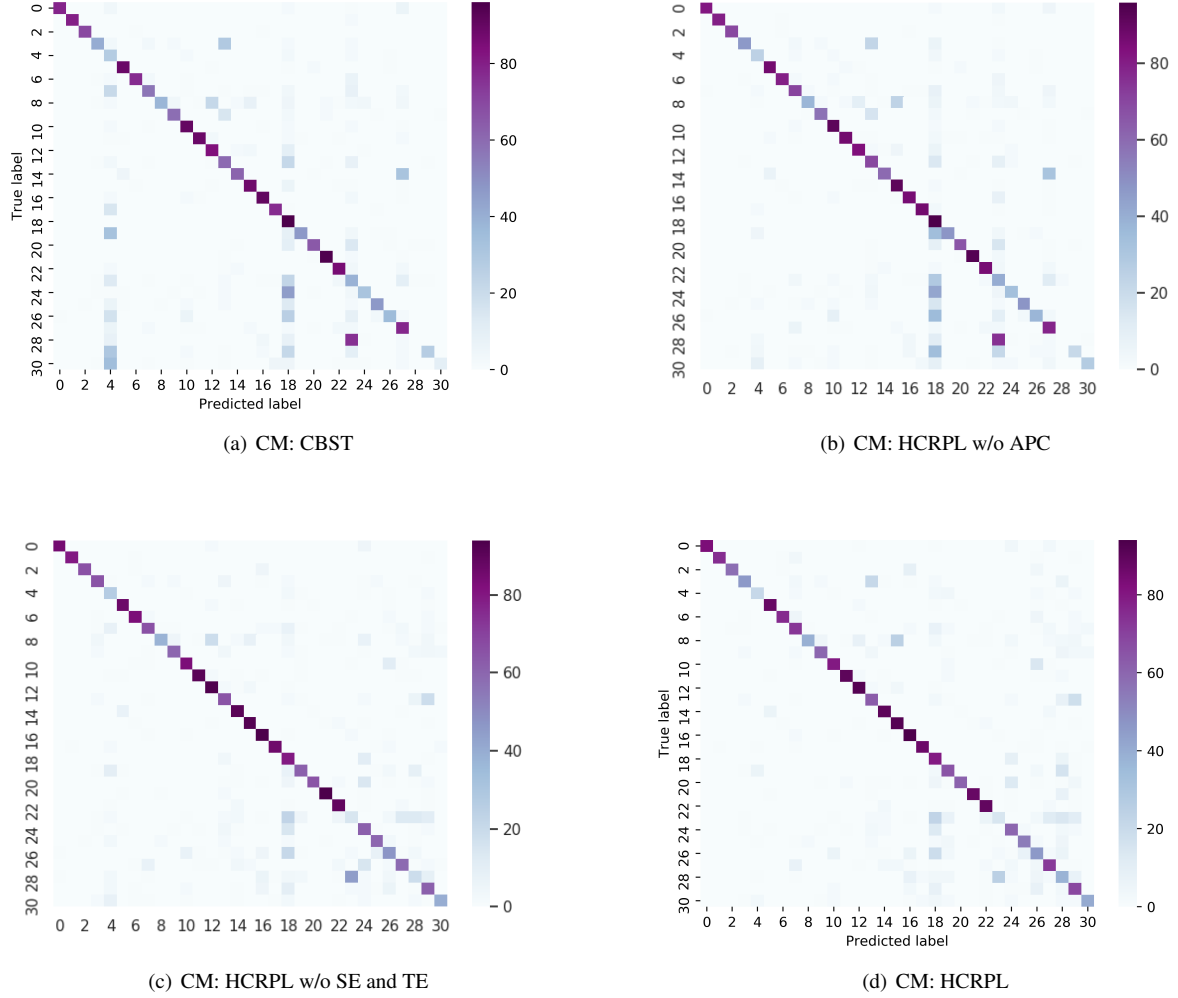


Figure 5: (a)-(d) The Confusion Matrix (CM) visualization for CBST, HCRPL without APC, HCRPL without SE and TE and HCRPL. The result is obtained on Office-31 $W \rightarrow A$ under UDA setting using ResNet-50. To better visualize the results, we arrange the categories in alphabetic order.

tions and prevent the target samples belonging to the hard class to be misclassified into the other classes.

5.6.2. Focusing on the hard class.

As mention before, in many real applications, we pay more attention to the class with worst performance rather than the average accuracy. To measure the performance, we adopt recall, precision, and f1 score as metrics. We further analyze the result shown in Figure 5 and consider the class with worst performance, 'Stapler'. As shown in Figure 7, HCRPL obviously improves the recall of Stapler from 0.05 to 0.3 and the precision of Stapler from 0.2 to 0.37, which means that HCRPL reduces the probabilities of false positives and false negatives for hard class at the same time. The large improvement of these metrics indicates that HCRPL could be applied on more practical scenarios. Moreover, we observe more clearly that the APC is the main effect, and the SE and TE are the side effect to alleviate the hard class

problem. Meanwhile, the SE and TE could not alleviate the hard class problem alone and further work combining with APC.

5.6.3. Feature Visualization.

We train ResNet-50, CBST, and the proposed HCRPL on Office-31 $A \rightarrow W$ under UDA setting and plot the learned features with t-SNE [21] in Figure 6 (a-c), respectively. The purple and yellow points represent the learned features of the source domain and target domain, respectively. As mentioned in the section 1, pseudo-labeling is a promising paradigm for aligning and separating the class conditional distributions of various domains. Therefore, CBST and HCRPL could promote to learn target-discriminative representations and to align the class conditional distributions. Furthermore, HCRPL could learn more of the target-discriminative representations due to improving the accuracy of pseudo-labels.

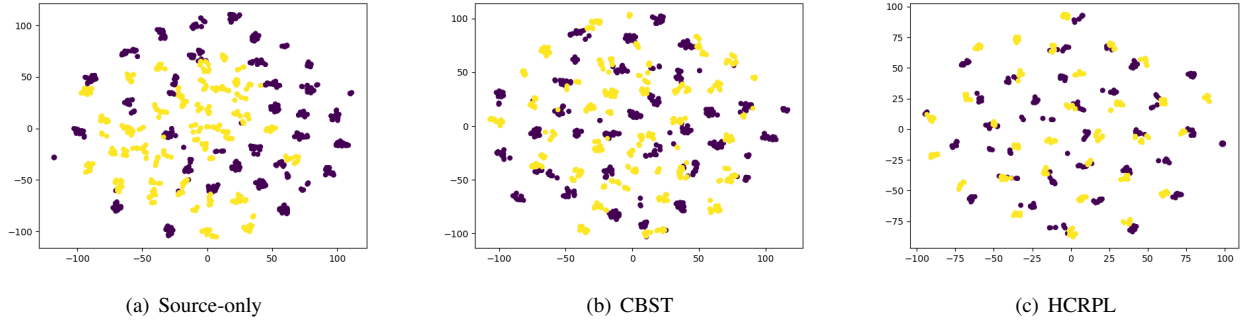


Figure 6: (a)-(c): The t-SNE visualization of features generated by Source-only, CBST, and HCRPL (purple: source, yellow: target). The result is obtained on Office-31 A \rightarrow W under UDA setting using ResNet-50.

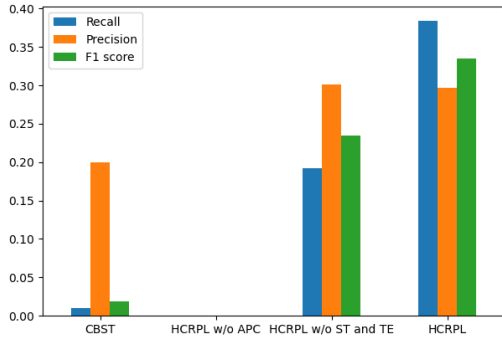


Figure 7: The recall, precision, and f1 score of class 'Stapler'. the recall, precision, and f1 score of HCRPL w/o APC are 0, since no target samples belonging to class 'Stapler' is classified correctly.

5.6.4. Convergence.

The convergence of ResNet, CBST, and the proposed HCRPL can be demonstrated by the error rates in the target domain on Office-31 A \rightarrow W under UDA setting. As shown in Figure 8, the following observations can be made: 1) CBST and HCRPL are more stable than ResNet (baseline) due to alleviating overfitting to the source domain. 2) The target error decreases gradually learnt by CBST and HCRPL because the pseudo-labeling methods progressively generate more pseudo-labels and learn more of the target-discriminative representations as the training progresses. 3) The disparity of the target error between CBST and HCRPL increases gradually, which indicates that APC, SE, and TE effectively improve the accuracy of pseudo-labels.

6. Conclusions

Pseudo-labeling is a promising paradigm for solving the DA problem. However, false pseudo-labels greatly degrade its performance. To reduce the false pseudo-labels ratio, we first revealed the hard class problem existing in DA, which degrades the performance of DA and restricts the applica-

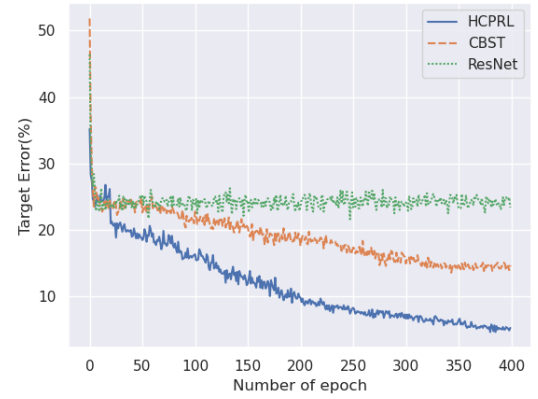


Figure 8: Test accuracy over iterations. The result is obtained on Office-31 A \rightarrow W under UDA setting using ResNet-50. ResNet means that we train the model without DA and only use the source domain as training data.

tion of DA. To alleviate the hard class problem, we proposed APC to calibrate predictions according to the difficulty degree for each class. Furthermore, we introduced SE and TE to improve the robustness of the predictions of target samples belonging to the hard class. In the experiment, we demonstrated that HCRPL achieved good results and outperformed some state-of-the-art methods with considerable margins under UDA setting. Meanwhile, HCRPL is suitable for the SSDA setting because it can learn target-discriminative representations. Experimental analysis shows that the proposed schemes can indeed alleviate the hard class problem and improve the accuracy of pseudo-labels.

References

- [1] Amodei, D., Ananthanarayanan, S., Anubhai, R., Bai, J., Zhu, Z., 2015. Deep speech 2: End-to-end speech recognition in english and mandarin. Computer Science.
- [2] Ben-David, S., Blitzer, J., Crammer, K., Kulesza, A., Pereira, F., Vaughan, J.W., 2010. A theory of learning from different domains. Machine Learning 79, 151–175.
- [3] Chen, C., Xie, W., Huang, W., Rong, Y., Ding, X., Huang, Y., Xu,

Table 6
Results on the Office-Home dataset under SSDA setting(%)

Network	Method	Ar Cl	Ar Pr	Ar Rw	Cl Ar	Cl Pr	Cl Rw	Pr Ar	Pr Cl	Pr Rw	Rw Ar	Rw Cl	Rw Pr	Avg
One-shot														
AlexNet	S+T	37.5	63.1	44.8	54.3	31.7	31.5	48.8	31.1	53.3	48.5	33.9	50.8	44.1
	DANN [8]	42.5	64.2	45.1	56.4	36.6	32.7	43.5	34.4	51.9	51.0	33.8	49.4	45.1
	ADR [29]	37.8	63.5	45.4	53.5	32.5	32.2	49.5	31.8	53.4	49.7	34.2	50.4	44.5
	CDAN [19]	36.1	62.3	42.2	52.7	28.0	27.8	48.7	28.0	51.3	41.0	26.8	49.9	41.2
	ENT [10]	26.8	65.8	45.8	56.3	23.5	21.9	47.4	22.1	53.4	30.8	18.1	53.6	38.8
	MME [27]	42.0	69.6	48.3	58.7	37.8	34.9	52.5	36.4	57.0	54.1	39.5	59.1	49.2
	CBST [46]	39.7	69.1	46	59.3	31.6	33.7	54.6	32.5	57.3	53.2	36.0	57.4	47.5
	HCRPL	46.0	73.3	48.8	63.8	38.7	38.4	58.1	37.4	59.7	61.0	40.1	62.2	52.3
VGG	S+T	39.5	75.3	61.2	71.6	37.0	52.0	63.6	37.5	69.5	64.5	51.4	65.9	57.4
	DANN [8]	52.0	75.7	62.7	72.7	45.9	51.3	64.3	44.4	68.9	64.2	52.3	65.3	60.0
	ADR [29]	39.7	76.2	60.2	71.8	37.2	51.4	63.9	39.0	68.7	64.8	50.0	65.2	57.4
	CDAN [19]	43.3	75.7	60.9	69.6	37.4	44.5	67.7	39.8	64.8	58.7	41.6	66.2	55.8
	ENT [10]	23.7	77.5	64.0	74.6	21.3	44.6	66.0	22.4	70.6	62.1	25.1	67.7	51.6
	MME [27]	49.1	78.7	65.1	74.4	46.2	56.0	68.6	45.8	72.2	68.0	57.5	71.3	62.7
	CBST [46]	42.2	78.9	62.2	75.0	39.5	52.8	70.6	40.4	73.2	68.8	54.1	70.7	60.7
	HCRPL	53.1	82.0	66.3	77.1	49.0	57.8	76.3	47.4	75.6	73.5	58.3	73.8	65.9
Three-shot														
AlexNet	S+T	44.6	66.7	47.7	57.8	44.4	36.1	57.6	38.8	57.0	54.3	37.5	57.9	50.0
	DANN [8]	47.2	66.7	46.6	58.1	44.4	36.1	57.2	39.8	56.6	54.3	38.6	57.9	50.3
	ADR [29]	45.0	66.2	46.9	57.3	38.9	36.3	57.5	40.0	57.8	53.4	37.3	57.7	49.5
	CDAN [19]	41.8	69.9	43.2	53.6	35.8	32.0	56.3	34.5	53.5	49.3	27.9	56.2	46.2
	ENT [10]	44.9	70.4	47.1	60.3	41.2	34.6	60.7	37.8	60.5	58.0	31.8	63.4	50.9
	MME [27]	51.2	73.0	50.3	61.6	47.2	40.7	63.9	43.8	61.4	59.9	44.7	64.7	55.2
	CBST [46]	45.3	72.6	48.4	62.3	40.3	37.3	64.2	40.7	61.6	58.6	39.9	62.6	52.8
	HCRPL	53.5	75.0	51.4	64.9	46.0	42.4	65.4	45.8	63.4	63.1	41.9	67.6	56.7
VGG	S+T	49.6	78.6	63.6	72.7	47.2	55.9	69.4	47.5	73.4	69.7	56.2	70.4	62.9
	DANN [8]	56.1	77.9	63.7	73.6	52.4	56.3	69.5	50.0	72.3	68.7	56.4	69.8	63.9
	ADR [29]	49.0	78.1	62.8	73.6	47.8	55.8	69.9	49.3	73.3	69.3	56.3	71.4	63.0
	CDAN [19]	50.2	80.9	62.1	70.8	45.1	50.3	74.7	46.0	71.4	65.9	52.9	71.2	61.8
	ENT [10]	48.3	81.6	65.5	76.6	46.8	56.9	73.0	44.8	75.3	72.9	59.1	77.0	64.8
	MME [27]	56.9	82.9	65.7	76.7	53.6	59.2	75.7	54.9	75.3	72.9	61.1	76.3	67.6
	CBST [46]	52.2	81.6	64.8	75.5	48.9	55.7	75.1	51.4	76.3	72.0	57.5	74.7	65.5
	HCRPL	59.7	84.7	68.7	78.5	55.3	61.7	77.6	55.5	78.6	76.1	62.2	79.0	69.8

- T., Huang, J., 2019a. Progressive feature alignment for unsupervised domain adaptation, in: Proceedings of the IEEE Conference on Computer Vision and Pattern Recognition, pp. 627–636.
- [4] Chen, D.D., Wang, Y., Yi, J., Chen, Z., Zhou, Z.H., 2019b. Joint semantic domain alignment and target classifier learning for unsupervised domain adaptation. arXiv preprint arXiv:1906.04053 .
- [5] Deng, W., Zheng, L., Jiao, J., 2018. Domain alignment with triplets. CoRR abs/1812.00893.
- [6] French, G., Mackiewicz, M., Fisher, M.H., 2018. Self-ensembling for visual domain adaptation, in: 6th International Conference on Learning Representations, OpenReview.net.
- [7] Ganin, Y., Lempitsky, V.S., 2015. Unsupervised domain adaptation by backpropagation, in: Bach, F.R., Blei, D.M. (Eds.), Proceedings of the 32nd International Conference on Machine Learning, JMLR.org. pp. 1180–1189.
- [8] Ganin, Y., Ustinova, E., Ajakan, H., Germain, P., Larochelle, H., Laviolette, F., Marchand, M., Lempitsky, V.S., 2016. Domain-adversarial training of neural networks. J. Mach. Learn. Res. 17, 59:1–59:35.
- [9] Goodfellow, I., Pouget-Abadie, J., Mirza, M., Xu, B., Warde-Farley, D., Ozair, S., Courville, A., Bengio, Y., 2014. Generative adversarial nets, in: Advances in neural information processing systems, pp. 2672–2680.
- [10] Grandvalet, Y., Bengio, Y., 2005. Semi-supervised learning by entropy minimization, in: Advances in neural information processing systems, pp. 529–536.
- [11] Gretton, A., Borgwardt, K.M., Rasch, M.J., Schölkopf, B., Smola, A.J., 2012. A kernel two-sample test. J. Mach. Learn. Res. 13, 723–773.
- [12] He, K., Zhang, X., Ren, S., Sun, J., 2016. Deep residual learning for image recognition, in: Proceedings of the IEEE conference on computer vision and pattern recognition, pp. 770–778.
- [13] Krizhevsky, A., Sutskever, I., Hinton, G.E., 2012. Imagenet classification with deep convolutional neural networks, in: Bartlett, P.L., Pereira, F.C.N., Burges, C.J.C., Bottou, L., Weinberger, K.Q. (Eds.), Advances in Neural Information Processing Systems, pp. 1106–1114.
- [14] Laine, S., Aila, T., 2017. Temporal ensembling for semi-supervised learning, in: 5th International Conference on Learning Representations, ICLR, OpenReview.net.
- [15] LeCun, Y., Bengio, Y., Hinton, G., 2015. Deep learning. nature 521,

- 436–444.
- [16] Lee, D.H., 2013. Pseudo-label: The simple and efficient semi-supervised learning method for deep neural networks, in: Workshop on challenges in representation learning, ICML, p. 2.
 - [17] Li, J., Chen, E., Ding, Z., Zhu, L., Lu, K., Huang, Z., 2019. Cycle-consistent conditional adversarial transfer networks, in: Proceedings of the 27th ACM International Conference on Multimedia, pp. 747–755.
 - [18] Long, M., Cao, Y., Wang, J., Jordan, M.I., 2015. Learning transferable features with deep adaptation networks, in: Bach, F.R., Blei, D.M. (Eds.), Proceedings of the 32nd International Conference on Machine Learning, JMLR.org. pp. 97–105.
 - [19] Long, M., Cao, Z., Wang, J., Jordan, M.I., 2018. Conditional adversarial domain adaptation, in: Advances in Neural Information Processing Systems, pp. 1640–1650.
 - [20] Long, M., Zhu, H., Wang, J., Jordan, M.I., 2017. Deep transfer learning with joint adaptation networks, in: ICML.
 - [21] Maaten, L.v.d., Hinton, G., 2008. Visualizing data using t-sne. Journal of machine learning research 9, 2579–2605.
 - [22] Motiian, S., Piccirilli, M., Adjero, D.A., Doretto, G., 2017. Unified deep supervised domain adaptation and generalization, in: Proceedings of the IEEE International Conference on Computer Vision, pp. 5715–5725.
 - [23] Pan, S.J., Yang, Q., 2009. A survey on transfer learning. IEEE Transactions on knowledge and data engineering 22, 1345–1359.
 - [24] Purushotham, S., Carvalho, W., Nilanon, T., Liu, Y., 2017. Variational recurrent adversarial deep domain adaptation, in: 5th International Conference on Learning Representations, OpenReview.net.
 - [25] Qin, C., Wang, L., Ma, Q., Yin, Y., Wang, H., Fu, Y., 2020. Opposite structure learning for semi-supervised domain adaptation. arXiv preprint arXiv:2002.02545.
 - [26] Saenko, K., Kulis, B., Fritz, M., Darrell, T., 2010. Adapting visual category models to new domains, in: ECCV, Springer.
 - [27] Saito, K., Kim, D., Sclaroff, S., Darrell, T., Saenko, K., 2019. Semi-supervised domain adaptation via minimax entropy. CoRR abs/1904.06487.
 - [28] Saito, K., Ushiku, Y., Harada, T., 2017. Asymmetric tri-training for unsupervised domain adaptation, in: Proceedings of the 34th International Conference on Machine Learning-Volume 70, JMLR. org. pp. 2988–2997.
 - [29] Saito, K., Ushiku, Y., Harada, T., Saenko, K., 2018a. Adversarial dropout regularization, in: 6th International Conference on Learning Representations, OpenReview.net.
 - [30] Saito, K., Watanabe, K., Ushiku, Y., Harada, T., 2018b. Maximum classifier discrepancy for unsupervised domain adaptation, in: Proceedings of the IEEE Conference on Computer Vision and Pattern Recognition, pp. 3723–3732.
 - [31] Shao, R., Lan, X., Yuen, P.C., 2018. Feature constrained by pixel: Hierarchical adversarial deep domain adaptation, in: Proceedings of the 26th ACM international conference on Multimedia, pp. 220–228.
 - [32] Simonyan, K., Zisserman, A., 2015. Very deep convolutional networks for large-scale image recognition, in: Bengio, Y., LeCun, Y. (Eds.), 3rd International Conference on Learning Representations.
 - [33] Sun, B., Feng, J., Saenko, K., 2016. Return of frustratingly easy domain adaptation, in: Thirtieth AAAI Conference on Artificial Intelligence.
 - [34] Sun, B., Saenko, K., 2016. Deep CORAL: correlation alignment for deep domain adaptation, in: Hua, G., Jégou, H. (Eds.), Computer Vision - ECCV 2016 Workshops, pp. 443–450.
 - [35] Szegedy, C., Zaremba, W., Sutskever, I., Bruna, J., Erhan, D., Goodfellow, I.J., Fergus, R., 2014. Intriguing properties of neural networks, in: Bengio, Y., LeCun, Y. (Eds.), 2nd International Conference on Learning Representations.
 - [36] Tang, H., Jia, K., 2019. Discriminative adversarial domain adaptation. arXiv preprint arXiv:1911.12036.
 - [37] Tarvainen, A., Valpola, H., 2017. Mean teachers are better role models: Weight-averaged consistency targets improve semi-supervised deep learning results, in: 5th International Conference on Learning Representations, OpenReview.net.
 - [38] Tzeng, E., Hoffman, J., Zhang, N., Saenko, K., Darrell, T., 2014. Deep domain confusion: Maximizing for domain invariance. arXiv preprint arXiv:1412.3474.
 - [39] Venkateswara, H., Eusebio, J., Chakraborty, S., Panchanathan, S., 2017. Deep hashing network for unsupervised domain adaptation, in: Proceedings of the IEEE Conference on Computer Vision and Pattern Recognition, pp. 5018–5027.
 - [40] Xie, S., Zheng, Z., Chen, L., Chen, C., 2018. Learning semantic representations for unsupervised domain adaptation, in: Dy, J.G., Krause, A. (Eds.), Proceedings of the 35th International Conference on Machine Learning, PMLR. pp. 5419–5428.
 - [41] Xu, R., Li, G., Yang, J., Lin, L., 2019. Larger norm more transferable: An adaptive feature norm approach for unsupervised domain adaptation, in: Proceedings of the IEEE International Conference on Computer Vision, pp. 1426–1435.
 - [42] Zhang, C., Bengio, S., Hardt, M., Recht, B., Vinyals, O., a. Understanding deep learning requires rethinking generalization, in: 5th International Conference on Learning Representations.
 - [43] Zhang, Y., Liu, T., Long, M., Jordan, M.I., b. Bridging theory and algorithm for domain adaptation, in: Chaudhuri, K., Salakhutdinov, R. (Eds.), Proceedings of the 36th International Conference on Machine Learning.
 - [44] Zhang, Y., Tang, H., Jia, K., Tan, M., 2019. Domain-symmetric networks for adversarial domain adaptation, in: Proceedings of the IEEE Conference on Computer Vision and Pattern Recognition, pp. 5031–5040.
 - [45] Zou, Y., Yu, Z., Liu, X., Kumar, B., Wang, J., 2019. Confidence regularized self-training, in: Proceedings of the IEEE International Conference on Computer Vision, pp. 5982–5991.
 - [46] Zou, Y., Yu, Z., Vijaya Kumar, B., Wang, J., 2018. Unsupervised domain adaptation for semantic segmentation via class-balanced self-training, in: Proceedings of the European conference on computer vision (ECCV), pp. 289–305.